Phase Equilibria and the Thermodynamics of Coexisting Phases in the System Iron–Lithium–Oxygen*

YU. D. TRETYAKOV, N. N. OLEYNIKOV, YU. G. METLIN, AND A. P. ERASTOVA

Department of Chemistry, Moscow State University, Moscow, USSR

Phase equilibria in the system Fe_2O_3–FeO–$Li_{0.5}Fe_{0.5}O$ have been studied over a broad range of temperatures (900–1200°C) and partial pressure of oxygen (10^{-15} – 1 atm) both by quench methods and solid-electrolyte electromotive force measurements together with chemical and X-ray analyses. Equilibrium conditions have been determined for the formation of iron lithium spinel, $Li_xFe_{3-x}O_{4+y}$, which changes its non-stoichiometric character according to the amount of oxygen present from an excess of the latter ($y > 0$) when $x \approx 0$ to a deficit ($y < 0$) when x approaches 0.5. The activity of the components in coexisting spinel and wüstite phases has been calculated. It is shown that solutions of lithium ferrite with magnetite in equilibrium with wüstite are characterized by small deviations from ideality—positive in the region which is rich in magnetite and negative in the concentration range bordering on lithium ferrite. Furthermore, ΔH is approximately zero, i.e., the solutions are athermal. Solutions of lithium ferrite and magnetite in equilibrium with hematite and solutions of wüstite and lithium orthoferrite in equilibrium with the spinel phase are characterized by marked deviations from ideality.

Introduction

Among the ferrites with spinel structure special attention is given to the formation of a polycrystalline lithium ferrite with a square hysteresis loop having a highest Curie point of 670°C (*1*) and retaining its superstructure up to 750°C (*2*). In spite of numerous investigations designed to establish the synthesis conditions, the kinetics of formation, and the thermal working of the lithium-containing ferrites (*3–8*), many peculiarities of the behavior have not been satisfactorily explained. It is known, for example, that the squareness of the hysteresis loop of lithium-containing ferrites is extremely sensitive to the value of the oxygen partial pressure at the thermal working conditions. However, it is not clear whether this phenomenon is related to phase decomposition of spinel (*6*) or to a change in the concentration of point defects within the limits of a monophase area (*9*).

The solution of this and a series of related problems should contribute to the understanding of phase equilibria and thermodynamic properties of coexisting phases in the Fe–Li–O system. The clarification of the equilibrium conditions for formation of iron–lithium spinel, particularly the dependence of nonstoichiometry on the oxygen partial pressure and temperature, obviously presents considerable interest. Data in the literature on phase equilibria in the Fe–Li–O system give little information. From Refs. (*6* and *7*), it follows that in the Fe–Li–O system it is possible to have formation of two phases of variable composition: one with spinel structure, the other with NaCl structure. The first of these is a solid solution based on magnetite $Li_xFe_{3-x}O_{4+y}$ ($0 < x \leqslant 0.5$); the second, a solution based on wüstite $Li_zFe_{1-z}O_{1+\delta}$ ($0 < z \leqslant 0.5$). According to the data in Ref. (*7*), decomposition of the spinel phase leads to formation of a wüstite solution richer in lithium than the spinel. Relatively recently (*10*) the existence of yet another compound, $LiFe_5O_8$, in the binary system Li_2O–Fe_2O_3 has been established.

The scope of the present investigation was limited to the study of phase equilibria in the

---

* Original manuscript received in Russian. A copy is available on written request to the editors.

high-oxygen regions of the Fe–Li–O diagram and to the determination of the thermodynamic properties of the coexisting phases.

Experimental Part

For studying the phase equilibria two procedures were used:

(a) quenching specimens after equilibration with gas phase having a particular partial pressure of oxygen;

(b) an electromotive force method using a solid electrolyte with purely anionic-oxygen conductivity.

Starting preparations. The starting oxide mixtures for the investigation of equilibria by the quench method were obtained from lithium orthoferrite and hematite, taken in the proportions shown in Table I and homogenized by heating for 2 hr at 900°C. The orthoferrite, in its turn, was prepared according to the reaction

$$Li_2CO_3 + Fe_2O_3 = 2LiFeO_2 + CO_2, \quad (1)$$
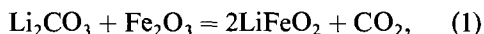
by heating at 700°C for 3 hr. This use of orthoferrite as an intermediate enabled us to reduce significantly the loss of lithium during the process of preparing the starting preparations (3).

TABLE I

COMPOSITION OF STARTING OXIDE MIXTURES FOR INVESTIGATING THE EQUILIBRIA BY THE DYNAMIC METHOD

N_{LiFeO_2}	$N_{Fe_2O_3}$	x in formula $Li_xFe_{3-x}O_{4+y}$
0.025	0.975	0.0375
0.050	0.950	0.0750
0.075	0.925	0.1125
0.100	0.900	0.1500
0.125	0.875	0.1875
0.150	0.850	0.2250
0.200	0.800	0.3000
0.250	0.750	0.3750
0.267	0.733	0.4000
0.283	0.717	0.4250
0.300	0.700	0.4500
0.317	0.683	0.4750
0.333	0.667	0.5000
0.400	0.600	0.6000
0.500	0.500	0.7500
0.700	0.300	1.0500
0.800	0.200	1.2000
0.900	0.100	1.3500

For investigating the phase equilibria using the EMF method, several series of samples were prepared:

1. Samples with overall composition $Li_zFe_{1-z}O_{1+\delta}$, where $z = 0, 0.12, 0.24, 0.36, 0.50$ and $\delta = 0.13, 0.09, 0.06, 0.03, 0$, respectively, were obtained from lithium orthoferrite, hematite and "FeO" by the reaction:

$$zLiFeO_2 + (1 - 2z - 2\delta)FeO + \delta Fe_2O_3 = Li_zFe_{1-z}O_{1+\delta}. \quad (2)$$
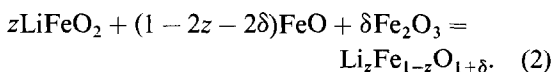
2. Samples of the composition $Li_tFe_{4-t}O_5$, where $t = 0, 0.14, 0.28, 0.42, 0.56, 0.70, 0.84, 1.00$, were obtained by the reaction:

$$tLiFeO_2 + 2(1 - t)FeO + Fe_2O_3 = Li_tFe_{4-t}O_5. \quad (3)$$
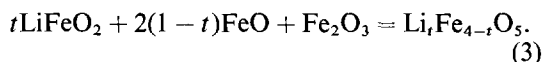
3. Samples of the composition $Li_xFe_{3-x}O_{3.99}$, where $x = 0, 0.07, 0.14, 0.20, 0.27, 0.34, 0.42, 0.50$, were obtained from lithium ferrite and magnetite by the reaction:

$$2xLi_{0.5}Fe_{2.5}O_{3.99} + (1 - 2x)Fe_3O_{3.99} = Li_xFe_{3-x}O_{3.99}. \quad (4)$$
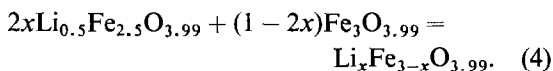
4. Samples of the composition $Li_yFe_{5-y}O_7$, where $y = 0, 0.07, 0.14, 0.20, 0.27, 0.34, 0.43, 0.50$, were obtained from lithium orthoferrite, hematite and FeO by the reaction:

$$yLiFeO_2 + (1 - 2y)FeO + 2Fe_2O_3 = Li_yFe_{5-y}O_7 \quad (5)$$
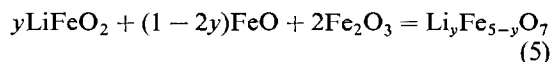
Wüstite of the composition "FeO" and magnetite "$Fe_3O_{3.99}$" were prepared in turn from carbonyl iron and hematite, mixtures of which were pressed into pellets ($P = 1.6$ T/cm^2) and heated in evacuated quartz ampoules at 900°C for a period of 24 hr. Chemical analysis of the reaction products for Fe^{2+} and Fe^{3+} confirmed the presence of wüstite and magnetite of the required composition.

Lithium ferrite was obtained from hematite and lithium orthoferrite by reacting the powder mixture, which was carefully mixed in an agate mortar under a layer of ether for 2 hr, at a temperature of 900°C and a partial pressure of oxygen of 0.016 atm. for 20 hr.

Reactions (2)–(5) were carried out on pelletized mixtures at 900°C for 24 hr in evacuated quartz ampoules. For carrying out reactions (3) and (4) at 1100°C, double quartz ampoules were used with metal titanium chips in the space between. The titanium precluded any possible oxidation of the specimens in the inner ampoule as a result of air flow from the outside.

Investigation of equilibria by the quench method
(11, 12). The setup for investigating equilibria by
the quench method is shown schematically in
Fig. 1. The platinum container (1) with an 0.6-g
specimen is attached to a special suspension (2)
in the center of the quartz reactor (3), which in
turn is placed in a vertical furnace (4). The
construction of the furnace permitted 4 reactors
to be in place simultaneously. The specimens
were heated at constant temperature in a gas
medium with fixed oxygen partial pressure for the
period of time needed to attain equilibrium
between the gas and condensed phases. After the
burning through of the suspension filament (5),
the specimens were quenched by being dropped
into receiver (6), containing liquid nitrogen.
The temperature in the zone of the oxides was
measured with a Pt–Pt/Rh thermocouple (7).
On the basis of preliminary experiments the times
selected for holding the specimens isothermally
to guarantee establishment of equilibrium be-
tween gas and condensed phases were as follows:
900°C, 20 hr; 1000°C, 10 hr; 1100°C, 6 hr;
1200°C, 4 hr.

Experiments were carried out in gas mixtures
having oxygen partial pressures of 1, 0.21, 0.016,
and 0.001 atm as well as with the oxygen partial

pressure created by the thermal dissociation of
carbon dioxide. The oxygen content of all the gas
mixtures was determined by measurement of the
EMF of a cell with divided gas space:

gas mixture
with measured $(Pt)|ZrO_2(CaO)|(Pt)$, air.
pressure of oxygen   (6)
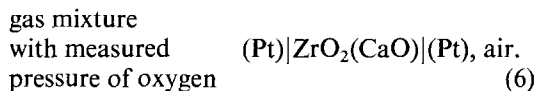
All the gas mixtures used were dried with
concentrated sulfuric acid together with granu-
lated anhydrous $Mg(ClO_4)_2$. The latter was
contained in three consecutively connected
drying columns. Such precautions were taken
because even small amounts of water vapor in the
gas phase are enough to give nonequilibrium
removal of lithium oxide from the condensed
phase in the form of LiOH *(13).*

Phase analysis of the quenched specimens
was carried out by X-rays using Debye's method
with FeK_α radiation. Lattice constants were
determined photographically and on a diffracto-
meter with a possible error of ±0.001 Å.

As has been shown earlier *(14),* for composi-
tions $Li_xFe_{3-x}O_{4+\gamma}$ the quantity γ can be deter-
mined by the formula

$$\gamma = \frac{1}{2}\frac{1 - 2x - pM}{1 + 8p},\qquad(7)$$

where p is the number of gram-ions of Fe^{2+} in
1 g of the dissolved condensed phase and M is
the "molecular weight" of the composition
$Li_xFe_{3-x}O_4$ $(\gamma = 0)$. In order to preclude oxida-
tion of the Fe^{2+}, the quenched specimens were
brought to solution in sealed glass ampoules
filled with an inert atmosphere. The determination
of the Fe^{2+} content was done by potentiometric
titration with a solution of cerium(IV) sulfate.

Investigation of equilibria by the EMF method.
To determine the chemical potential of oxygen
in coexisting spinel and wüstite phases the EMF
method was used with a solid electrolyte
$ZrO_2(CaO)$ having anion-oxygen conductivity.
The construction of the cells with divided and
strictly defined space over the electrodes has been
described by one of the authors *(15).* The basic
feature of the cells used (Fig. 2) is the tube (1), a
gas-impermeable tube of zirconium dioxide
stabilized with calcium oxide. The tube serves
as an electrolyte with oxygen conductivity and at
the same time as a working chamber that separ-
ates the electrode being investigated (3) from the
standard (2). The powdered specimen was placed
in the platinum container (3), which served sim-
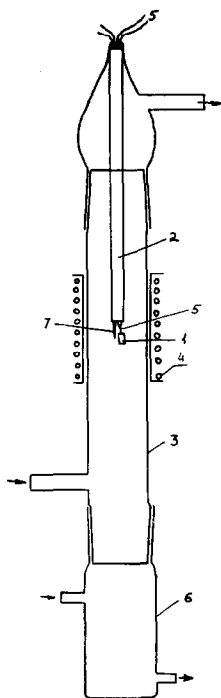ultaneously as the inner electrode. To eliminate

FIG. 1. Diagram of the apparatus for investigating
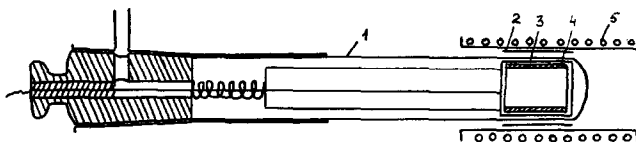equilibria by the quench method.

FIG. 2. Diagram of the cell with divided electrode space for measurement of the electromotive force.

contact potentials, the sample was insulated from the platinum electrode by the corundum cup (4). After introduction of the specimen into the working chamber, the latter was evacuated to a residual pressure of 10^{-3} mm Hg, flushed, and finally filled with pure helium.

For investigating the specimens of $Li_t Fe_{4-t}O_5$ where $t = 0.70$ and 0.34, air was used as the comparison electrode; for investigating the specimens of $Li_t Fe_{4-t}O_5$ where $t = 0$, 0.14, 0.33, 0.42 and 0.56, equilibrium mixtures of FeO/Fe_3O_4 served as the electrode. Experiments were carried out over the interval 800–1000°C.

The chemical potential of the oxygen over the coexisting phases was calculated from the equilibrium values of the EMF by well-known thermodynamic relations. For the electro-chemical elements:

standard oxygen-containing electrode,	(Pt)	solid electrolyte	(Pt),	investigated oxygen-containing electrode

the electromotive force is given by

$$E = \frac{1}{4F} \int_{\mu'_{O_2}}^{\mu''_{O_2}} t_{ion}\, d\mu_{O_2}, \qquad (8)$$

where μ'_{O_2} and μ''_{O_2} are the chemical potentials of the oxygen on the two sides of the electrolyte, F is the Faraday number, and t_{ion} is the transport number of the oxygen ions. If $t_{ion} = 1$, then from Eq. (8) it follows that

$$\mu''_{O_2} - \mu'_{O_2} + 4EF, \qquad (9)$$

or with the substitution

$$\mu_{O_2} = \mu^0_{O_2} + RT \ln p_{O_2} \qquad (10)$$

we get

$$p''_{O_2} = p'_{O_2} \exp\left(\frac{4EF}{RT}\right) \qquad (11)$$

where p'_{O_2} and p''_{O_2} are the equilibrium oxygen pressures over the reference and investigated electrodes, respectively.

Basic Results and Discussion

The results of investigating phase equilibria by the quench method are represented in Figs. 3–6 (chemical analysis data) as well as in Figs. 7 and 8 (X-ray analysis data). It is easy to see that the specimens of overall composition $Li_x Fe_{3-x} O_{4+\gamma}$ over the range of temperature (900–1200°C) and oxygen partial pressure studied fall into 3 groups:

a. Two-phase mixtures of hematite and spinel. On the $\gamma = f(x)$ curves, the rectilinear sections originating from the points with $\gamma = 0.5$ and $x = 0$ correspond to these mixtures. These straight lines are actually tie-lines of coexisting phases, one of which is pure hematite and the other is iron–lithium spinel of a variable composition given by the point of intersection of the tie-line with the abscissa axis. On the $a = f(x)$ curves, the two-phase mixtures of hematite and spinel correspond to the rectilinear segments parallel to the abscissa axis; these characterize the invariability of the spinel composition along the individual tie-lines.
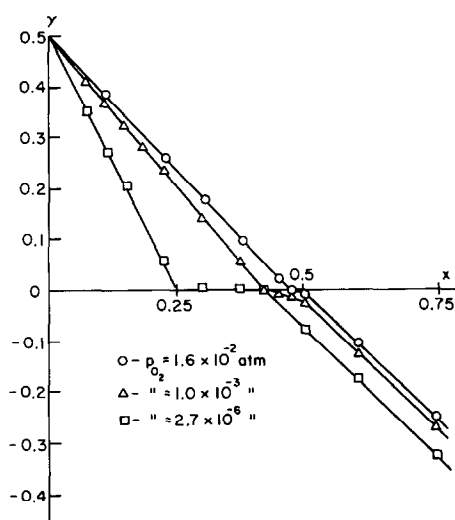
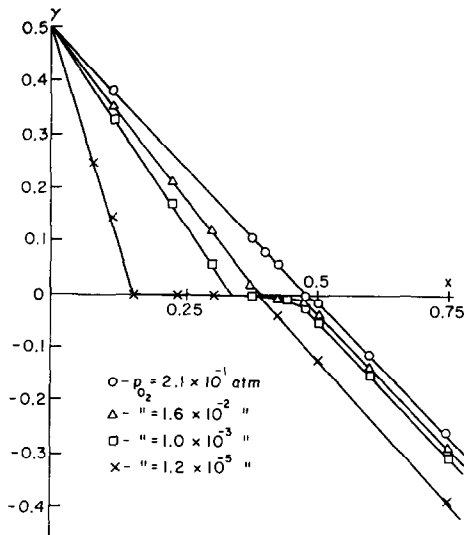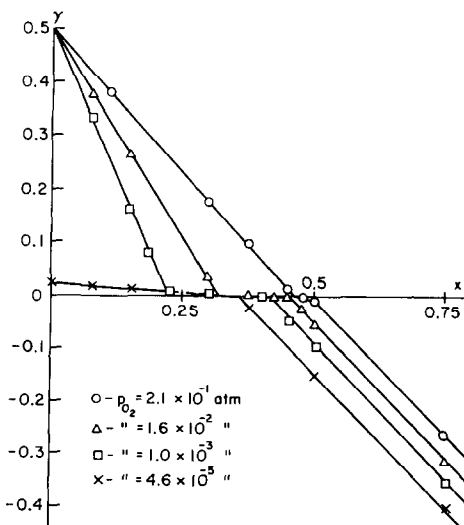FIG. 3. Dependence of $\gamma = f(x)$ in $Li_x Fe_{3-x} O_{4+\gamma}$ at 900°C.

FIG. 4. Dependence of $\gamma = f(x)$ in $Li_xFe_{3-x}O_{4+\gamma}$ at 1000°C.

b. Single-phase iron–lithium spinel of variable composition.

The curvilinear sections on the $\gamma = f(x)$ diagrams (Fig. 3–6) and the sharp change in lattice constant as a function of x (Figs. 7 and 8) correspond to this phase. It is noteworthy that the range of composition (value of x) corresponding to the single-phase spinel increases in proportion to an increase in temperature. Furthermore, the oxygen nonstoichiometry of the spinel changes its character with different values of x. For compositions close to pure lithium ferrite,

FIG. 6. Dependence of $\gamma = f(x)$ in $Li_xFe_{3-x}O_{4+\gamma}$ at 1200°C.

$Li_{0.5}Fe_{2.5}O_4$, the spinel phase has a deficit of oxygen, whereas compositions rich in iron are characterized by an excess of oxygen, the latter reaching its maximum value at pure magnetite ($x = 0$).

c. Two-phase mixtures of spinel and wüstite phases of variable composition.

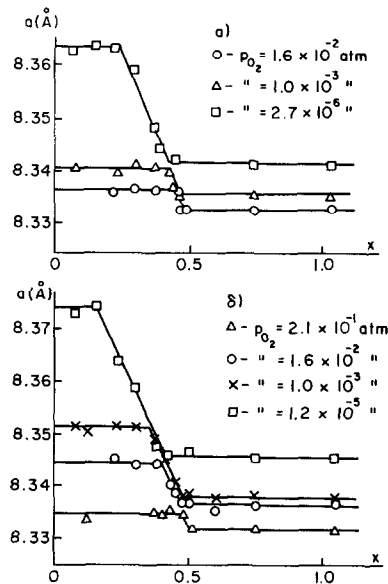On the $\gamma = f(x)$ curves (Figs. 3–6), the rectilinear sections (tie-lines

FIG. 5. Dependence of $\gamma = f(x)$ in $Li_xFe_{3-x}O_{4+\gamma}$ at 1100°C.

FIG. 7. Dependence of $a = f(x)$ for the compositions $Li_xFe_{3-x}O_{4+\gamma}$ at (a) 900°C and (b) 1000°C.
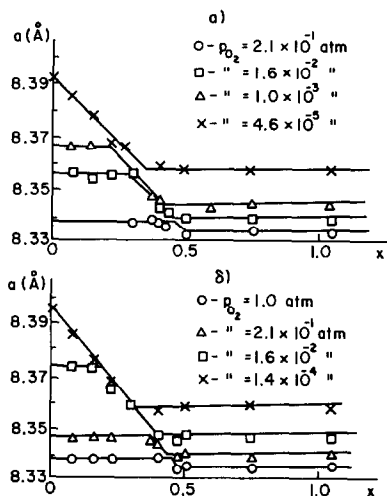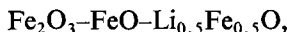
FIG. 8. Dependence of $a = f(x)$ for the compositions $Li_xFe_{3-x}O_{4+\gamma}$ at (a) 1100°C and (b) 1200°C.

FIG. 9. Isothermal section of the state diagram for the system Fe_2O_3–FeO–$Li_{0.5}Fe_{0.5}O$ at 900°C. (●) $p_{O_2} = 2.7 \times 10^{-6}$ atm; (×) 1.0×10^{-3} atm; (△) 1.6×10^{-2} atm.

of coexisting phases) found below the axis of the abscissa correspond to these mixtures. In Figs. 7 and 8, which show the dependence $a = f(x)$, the rectilinear sections characterizing the invariability of spinel composition along the individual tie-lines correspond to mechanical mixtures of coexisting spinel and wüstite phases.

To construct the isothermal sections of the state diagram for the system

$$Fe_2O_3\text{–}FeO\text{–}Li_{0.5}Fe_{0.5}O,$$

the composition of the condensed phase $Li_xFe_{3-x}O_{4+\gamma}$ was calculated in mole percent (mole fraction) of the respective components according to the following formulas:

$$N_{Li_{0.5}Fe_{0.5}O} = \frac{2x}{2-\gamma}, \qquad (12)$$

$$N_{FeO} = \frac{1 - 2x - 2\gamma}{2 - \gamma}, \qquad (13)$$

$$N_{Fe_2O_3} = \frac{1 + \gamma}{2 - \gamma}. \qquad (14)$$

The results of these calculations are represented by the heavy lines in Figs. 9–12.

Inasmuch as the quench method did not allow us to map a significant portion of the two-phase spinel-wüstite region, the diagram was filled in with data obtained from the EMF method. To this end, the equilibrium oxygen pressures were measured for specimens of composition $Li_tFe_{4-t}O_5$ lying inside the two-phase region (broken lines in Figs. 9–11). Data from the X-ray
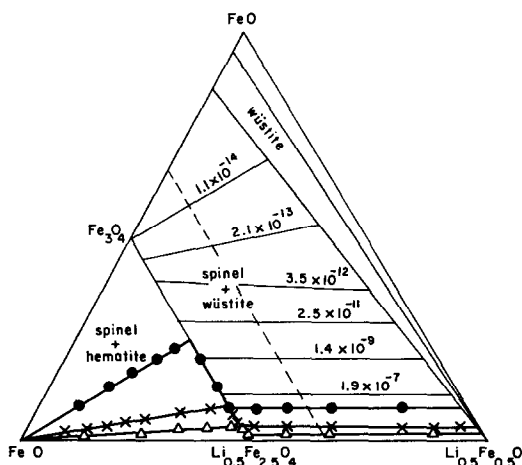
analysis confirmed the two-phase nature of the indicated specimens. Furthermore, comparison of the spinel constant with the base-line curve (Fig. 13) for specimens of compositions $Li_xFe_{1-z}O_{1+\gamma}$ and $Li_xFe_{3-x}O_{3.99}$ allowed us to fix the position of the tie-lines on the diagram (tie-lines are plotted with thin lines).

Some error in the determination of the position of the tie-lines can be related to the arbitrariness of the assumption that the spinel lattice constant at composition $Me_3O_{3.99}$ corresponds to that for the low-oxygen limit of the spinel field, the posi-
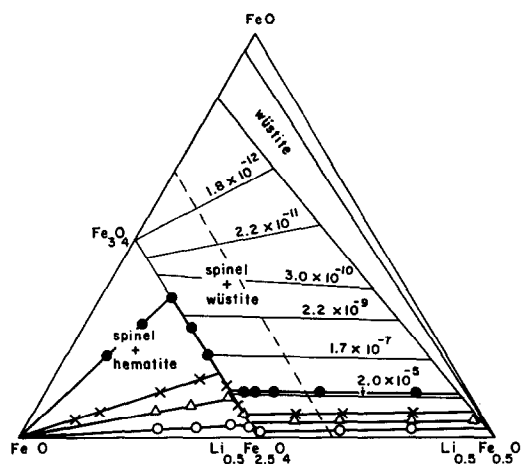

FIG. 10. Isothermal section of the state diagram for the system Fe_2O_3–FeO–$Li_{0.5}Fe_{0.5}O$ at 1000°C. (●) $p_{O_2} = 1.2 \times 10^{-5}$ atm; (×) 1.0×10^{-3} atm; (△) 1.6×10^{-2} atm; (○) 2.1×10^{-1} atm.
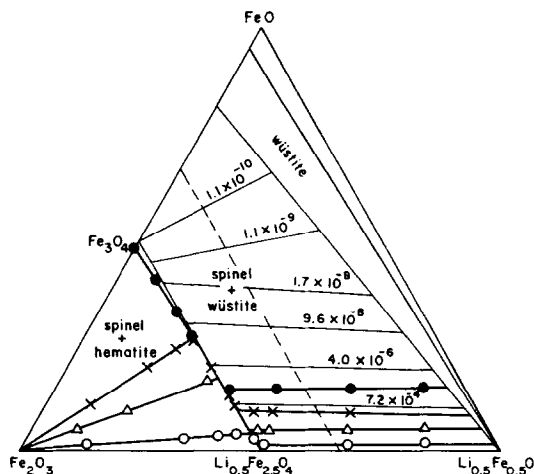
FIG. 11. Isothermal section of the state diagram for the system Fe_2O_3–FeO–$Li_{0.5}Fe_{0.5}O$ at 1100°C. (●) $p_{O_2} = 4.6 \times 10^{-5}$ atm; (×) 1.0×10^{-3} atm; (△) 1.6×10^{-2} atm; (○) 2.1×10^{-1} atm.

tion of which was established only for compositions rich in lithium. In order to convince ourselves of the insignificance of the error related to this assumption, we compared (Fig. 13) the spinel lattice constant for two series of compositions, $Li_xFe_{3-x}O_{3.99}$ and $Li_yFe_{5-y}O_7$, which lie along various sides of the one-phase spinel region. Within the limits of error at the temperatures chosen for the experiment, a change in the oxygen content of the spinel $Li_xFe_{3-x}O_{4+y}$ at constant x is not accompanied by a change in the lattice constant.
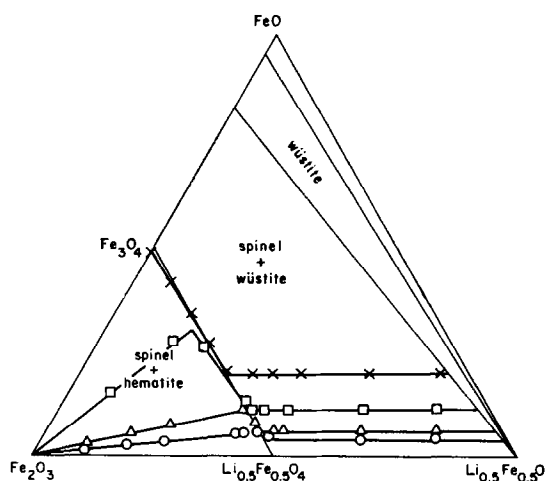

FIG. 12. Isothermal section of the state diagram for the system Fe_2O_3–FeO–$Li_{0.5}Fe_{0.5}O$ at 1200°C. (×) $p_{O_2} = 1.4 \times 10^{-4}$ atm; (□) 1.6×10^{-2} atm; (△) 2.1×10^{-1} atm; (○) 1.0 atm.
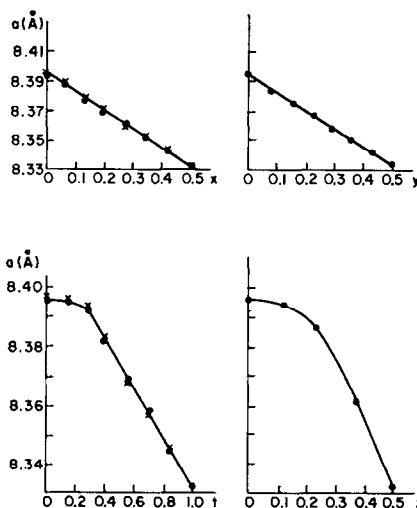
FIG. 13. Lattice parameter of compositions

$Li_xFe_{3-x}O_{3.99}$, $Li_yFe_{5-y}O_7$, $Li_tFe_{4-t}O_5$,

and $Li_zFe_{1-z}O_{1+\delta}$ at 900°C (●) and 1100°C (×).

The results of investigating the phase equilibria in the system Fe_2O_3–FeO–$Li_{0.5}Fe_{0.5}O$ were used for a thermodynamic analysis of the components in the various phases. As has been shown previously (16), the activity of any combination of components in the heterogeneous region of a system A–B–C can be calculated by the following formula:

$$\log a_{A_rB_sC_t} = -\frac{1}{j} \int_{(p_{C_j}^0)'}^{(p_{C_j}^0)''} \Delta d\log p_{O_2}$$

$$+ \frac{1}{j} \int_{(p_{C_j}^0)''}^{p_{C_j}} \frac{r(km - fn) + s(en - kl) + t(fl - em)}{fl - em}$$

$$\times d\log p_{C_j} \qquad (15)$$

Here $(p_{C_j}^0)'$ is the vapor pressure of component C over the phase $A_rB_sC_t$ that lies in the homogeneous region and $(p_{C_j}^0)''$ is the vapor pressure of component C over $A_rB_sC_{t+\Delta}$ that has the same relationship to components A and B as $A_rB_sC_t$ but is in equilibrium with another condensed phase. The first term of Eq. (15) characterizes the activity of $A_rB_sC_t$ in the phase $A_rB_sC_{t+\Delta}$ and the second takes into account the change in the activity of $A_rB_sC_t$ on integration along the two-phase boundary.

Equation (15) can be used for calculating the activity of any combination of components in any three-component system. For equilibrium

spinel and wüstite phases, the composition of which is expressed by the formulas $Li_xFe_{3-x}O_{4-\gamma}$ and $Li_zFe_{1-z}O_{1+\delta}$, i.e.,

$$e = x \qquad\qquad l = z$$
$$f = 3 - x \qquad m = 1 - z$$
$$k = 4 - \gamma \qquad n = 1 + \delta$$

the activities of magnetite ($r = 0$, $s = 3$, $t = 4$) and lithium ferrite ($r = 0.5$, $s = 2.5$, $t = 4$) can be calculated according to the formulas

$$\log a_{Fe_3O_4} = -\frac{1}{2} \int\limits_{(p^0_{O_2})_{FeO/Fe_3O_4}}^{p_{O_2}} \frac{x}{3z - x} \times (1 - 3\delta)\, d\log p_{O_2} \tag{16}$$

$$\log a_{Li_{0.5}Fe_{2.5}O_4} =$$
$$\frac{1}{4} \int\limits_{(p^0_{O_2})_{Li_{0.5}Fe_{0.5}O/Li_{0.5}Fe_{2.5}O_4}}^{p_{O_2}} \frac{1 - 2x}{3z - x} \times (1 - 3\delta)\, d\log p_{O_2} \tag{17}$$

taking into account that the oxygen nonstoichiometry is small ($\gamma = 0$) on the low-oxygen boundary of the spinel field.

The results of calculating the activities with Eqs. (16) and (17) are presented in Fig. 14. It is easy to see that the spinel solid solutions of lithium ferrite with magnetite in equilibrium with wüstite solid solutions are characterized by small deviations from ideality—positive in the region rich in magnetite and negative in the range of concentrations bordering on lithium ferrite. The character of the dependence $a_i = f(x)$ changes weakly with temperature; therefore,

$$\Delta H = \frac{\partial \ln a_i}{\partial (1/T)} = 0,$$
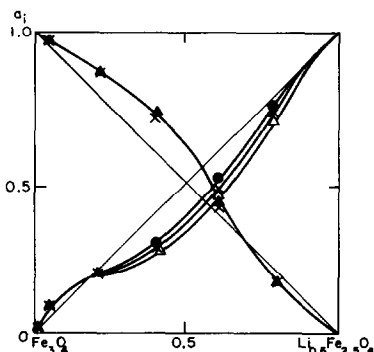
i.e., the solutions are athermal.

FIG. 14. Values of the activity of the components of spinel solution at the low-oxygen boundary. ($\triangle$) 900°C; ($\times$) 1000°C; ($\bullet$) 1100°C.
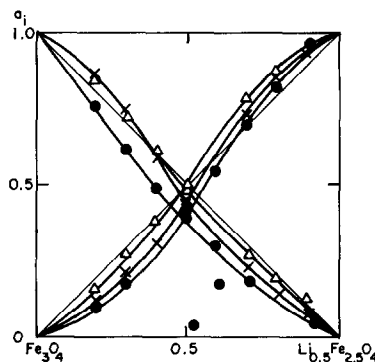

FIG. 15. Values of the activity of the components of spinel solution at the high oxygen boundary. ($\bullet$) 900°C; ($\times$) 1000°C; ($\triangle$) 1100°C.

Figure 15 gives the values of the activities of magnetite and lithium ferrite in the spinel phase, practically in equilibrium with pure hematite, as calculated by the formulas

$$\log a_{Fe_3O_4} =$$
$$-\frac{1}{2} \int\limits_{(p^0_{O_2})_{FeO/Fe_3O_4}}^{(p^0_{O_2})_{Fe_3O_4+\Delta/Fe_2O_3}} \Delta d\log p_{O_2}$$
$$-\frac{1}{4} \int\limits_{(p^0_{O_2})_{Fe_3O_4+\Delta/Fe_2O_3}}^{p_{O_2}} d\log p_{O_2}, \tag{18}$$

$$\log a_{Li_{0.5}Fe_{2.5}O_4} =$$
$$-\frac{1}{8} \int\limits_{(p^0_{O_2})_{Fe_2O_3/Li_{0.5}Fe_{2.5}O_4}}^{p_{O_2}} \frac{1 - 2x}{x} \times d\log p_{O_2} \tag{19}$$

It is evident that the solutions of lithium ferrite with magnetite, in equilibrium with hematite, have negative deviations from ideality over the entire range of concentration. As is to be expected, these deviations decrease with rise in temperature, so that at 1100°C the solutions are practically ideal. It is noteworthy that on going from the low-oxygen boundary to the high-oxygen boundary significant change (especially at 900°C) in the activity of the components of the spinel is accompanied by a negligibly small change in oxygen composition. The latter would not be detected by chemical analysis nor by measurement of lattice constant.

We have also calculated the activity of the components of wüstite solution coexisting with
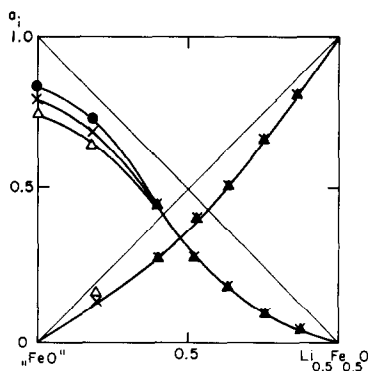
FIG. 16. Values of the activity of the components of wüstite solution found in equilibrium with spinel solid solution. (●) 900°C; (×) 1000°C; (△) 1100°C.

ponds to the pressure of oxygen over pure orthoferrite which is in equilibrium with the spinel phase. The quantity $(p_{O_2})_{Li_{0.5}Fe_{0.5}O}$ was obtained by extrapolating the $\Delta \bar{H}_{O_2} = f(z)$ curve to $z = 0.5$.

As shown in Fig. 16, solid solutions of $Li_{0.5}Fe_{0.5}O$ and $FeO_{1+\delta}$ are characterized by negative deviations from ideality, the magnitudes of which practically do not change with temperature (athermal solutions). As is to be expected in the binary system Fe–O in pure $Li_zFe_{1-z}O_{1+\delta}$ at $z = 0$, the activity of "FeO" is noticeably less than 1.0 and decreases with an increase in temperature. This is a consequence of the non-stoichiometry of wüstite, in equilibrium with magnetite, which increases with a rise in temperature.

spinel. Figure 16 shows the values of the activity of $Li_{0.5}Fe_{0.5}O$ and stoichiometric wüstite "FeO" calculated according to the following formulas:

$$\log a_{"FeO"} = -\frac{1}{2} \int_{(p_{O_2})_{"FeO"}}^{(p_{O_2})_{FeO_{1+\delta}}} \delta d\log p_{O_2}$$

$$-\frac{1}{2} \int_{(p_{O_2})_{FeO_{1+\delta}}}^{(p_{O_2})_{Li_zFe_{1-z}O_{1+\delta}}} \frac{z(1-\gamma) - x\delta}{3z - x} d\log p_{O_2} \qquad (20)$$

$$\log a_{Li_{0.5}Fe_{0.5}O} =$$

$$\frac{1}{4} \int_{(p_{O_2})_{Li_{0.5}Fe_{0.5}O}}^{(p_{O_2})_{Li_zFe_{1-z}O_{1+\delta}}} \left[\frac{(1-\gamma)(1-2z)}{3z - x} - \frac{8(3 - 2x)}{3z - x} \right] \times d\log p_{O_2}. \qquad (21)$$

In Eq. (20), $(p_{O_2})_{"FeO"}$ is the equilibrium oxygen pressure over the mixture of stoichiometric composition "FeO" $\rightleftarrows a$Fe $+ b$FeO$_{1+\delta'}$ $(p_{O_2})_{FeO_{1+\delta}}$ is the pressure of oxygen over wüstite in equilibrium with magnetite, and $(p_{O_2})_{Li_zFe_{1-z}O_{1+\delta}}$ is the pressure of oxygen over a wüstite phase of arbitrary composition in equilibrium with spinel. In Eq. (21), the lower limit of integration corres-

References

1. J. SMIT AND H. P. J. WIJN, "Ferrites." Wiley, New York (1959).
2. P. B. BROWN, Nature, 170, 1123 (1952).
3. E. W. GORTER, Pat. U.S.A., No. 2,751,357.
4. E. S. SAVRANSKAYA, Y. D. TRETYAKOV, AND A. P. ERASTOVA, Vest. Moscow Univ., No. 3 (1971).
5. A. J. POINTON AND R. C. SAULL, J. Amer. Ceram. Soc. 52, 157 (1969).
6. J. THERY, Ann. Chem. 7, 207 (1962).
7. D. W. STRICKLER AND R. ROY, J. Amer. Ceram. Soc. 44, 5 (1961).
8. A. HOFFMANN, Naturwissenschaften 26, 431 (1938).
9. V. A. GRANIK, Y. G. METLIN, N. N. OLEYNIKOV, AND Y. D. TRETYAKOV, Neorg. Mater. 7, 129 (1971).
10. G. DEMOISSAN AND C. GLEITZER, C.r. Acad. Sci. Ser. C 272, 458 (1971).
11. L. S. DARKEN AND R. W. GURRY, J. Amer. Chem. Soc. 67, 1398 (1945).
12. L. S. DARKEN AND R. W. GURRY, J. Amer. Chem. Soc. 68, 798 (1946).
13. A. E. VAN ARKEL, U. SPITSBERGEN, AND R. D. HEYDING, Can. J. Chem. 33, 446 (1955).
14. Y. D. TRETYAKOV AND N. N. OLEYNIKOV, J. Inorg. Chem. (USSR) 10, 1940 (1965).
15. Y. D. Tretyakov, Neorg. Mater. 1, 1928 (1965).
16. N. N. OLEYNIKOV AND Y. D. TRETYAKOV, Neorg. Mater. 5, 528 (1969).